Available online at www.sciencedirect.com
SCIENCE DIRECT®
European Journal of Medicinal Chemistry 39 (2004) 383–388
EUROPEAN JOURNAL OF MEDICINAL CHEMISTRY
www.elsevier.com/locate/ejmech

Preliminary communication

Quantitative structure activity relationship studies of diaryl furanones as selective COX-2 inhibitors

S. Shahapurkar [a], T. Pandya [a], N. Kawathekar [b], S.C. Chaturvedi [a,*]

[a] *School of Pharmacy, Devi Ahilya Vishwavidylaya, Takshashila Parisar, Khandwa Road, Indore, India*
[b] *Department of Pharmacy, SGSITS, Indore, India*

Received 4 April 2003; received in revised form 8 December 2003; accepted 15 December 2003

Abstract

Selective COX-2 inhibitors have attracted much attention in recent times in the design of non-steroidal anti-inflammatory agents (NSAID), which are devoid of the common side effects of classical NSAIDs. QSAR studies have been performed on a series of diaryl furanones that acts as selective COX-2 inhibitor using Molecular Operating Environment (MOE). The studies were carried out on 43 analogs. These studies produced good predictive models and give statistically significant correlations of selective COX-2 inhibitory with physical property, connectivity and conformation of molecule. Also when available COX-1 inhibitory data was analyzed with descriptors obtained from MOE, partial charge descriptor, van der Waal's surface area and solvation energy gave statistically significant results.

Keywords: NSAID; COX-2; QSAR

1. Introduction

Non-steroidal anti-inflammatory agents (NSAID) are widely used in the treatment and management of pain and inflammation. These compounds inhibit the enzyme cyclooxygenase (COX) and thus prevent the formation of prostaglandins at elevated levels causing inflammation [1]. It has been reported that selective inhibition of second isoform of the enzyme, cyclooxygenase-2 (COX-2) (induced during inflammation) may provide the therapeutic benefit without causing gastric ulceration associated with the classical agents [2]. The improved safety profile of COX-2 inhibitors may allow the use of these new agents for long-term prophylactic use in certain chronic diseases [3]. This has led intense efforts in search for potent and selective COX-2 inhibitors, as the next generation of anti-inflammatory agents. Several classes of compounds having selective COX-2 inhibitory activity have been reported in the literature for e.g. diaryl heterocylics as oxazoles [4], thiophens [5], pyrazoles [6], imidazoles [7], carbocycle [8], furanones [9] based inhibitors (Fig. 1) and those common classical agents modified to have selective COX-2 inhibitory activity as esters and amides of indomethacin [10], meclofenamic acid [11].

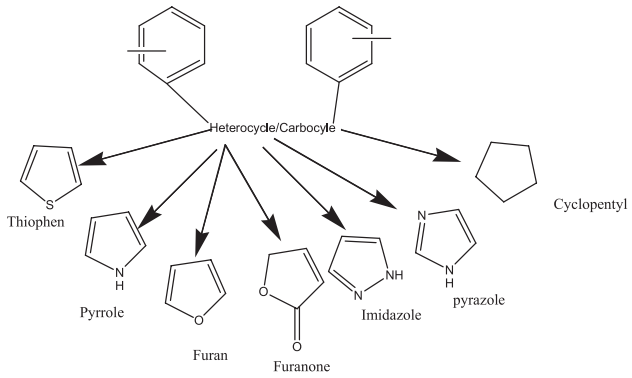

Fig. 1. Lead structures for selective COX-2 activity.

Thus our main objective is to design specific inhibitors of COX-2 in the hope that these molecules may be further explored as powerful non-ulcerogenic anti-inflammatory agents. A currently marketed product of selective COX-2 inhibitor category, Rofecoxib (4-(4′-methylsulphonylphenyl)-3-phenyl-2-(5H)-furanone, belongs to diaryl fura-

Abbreviations: COX-2, cyclooxygenase-2; MOE, Molecular Operating Environment; NSAID, non-steroidal anti-inflammatory agents; QSAR, quantitative structure activity relationships.

* Corresponding author.
E-mail address: sheetalvs@hotmail.com (S.C. Chaturvedi).

doi:10.1016/j.ejmech.2003.12.007

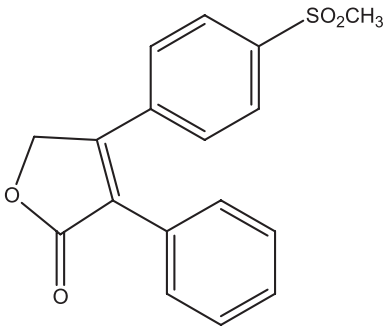

Fig. 2. Rofecoxib.

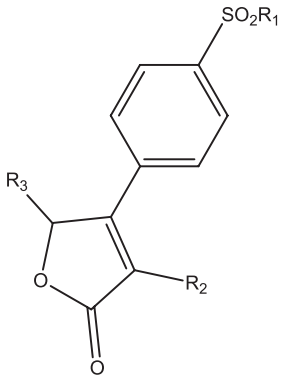

Fig. 3. Lead compound for the present study.

none category (Fig. 2). In view of this diaryl furanones [9] (Fig. 3) were selected for quantitative structure activity relationships (QSAR), for the present study. In addition nowhere quantitative structure activity analysis has been reported for diaryl furanones. Thus such studies may help for the design and synthesis of better selective COX-2 inhibitors.

2. Materials and methods

All computational work was performed on Pentium IV workstation-using software Molecular Operating Environment (MOE) developed by Chemical Computing Group Inc, Canada. A total of 43 compounds were selected for the present study. All the compounds were drawn on builder module of MOE. The compounds were then subjected to conformational analysis and energy minimization using stochastic conformation search with RMS gradient of 0.001 and iteration limit of 10 000 using a MMFF94 force field. The conformations available to a molecule have a dramatic effect on biological activity and reactivity. Thus the lowest energy conformer of all the compounds was transferred to database viewer and descriptors calculated. MOE calculates 193 descriptors from three classes—2D descriptor (use the atoms and connection information of the molecule for the calculation); i3D, internal 3D descriptors (use 3D coordinate information about each molecule and they are invariant to rotations and translations of the conformation) and x3D, external 3D descriptors, which use 3D, coordinate information but also require an absolute frame of reference. The correlation between the biological activity (pIC50) and the descriptors were performed by stepwise regression analysis using QSAR easy software [12]. Following statistical measures were used: N = number of samples, r = coefficient of correlation, F-test for quality of fit, t-test for test of significance, and s = standard deviation, S dep = standard error of prediction. Leave-one-out method was employed for cross-validation of the equation and q^2, cross-validated coefficient of correlation determined.

3. Result and discussion

The 43 compounds belonging to diaryl furanones category (Fig. 3) were divided into two sets, 31 compounds were taken in the training set (Table 1) and 12 compounds were taken in the test set (Table 2). The biological activities data for diaryl furanone derivatives were taken from literature [9]. The IC50 values for both COX-1 and COX-2 were transformed into –log[IC50*10^6] i.e. pIC50. Stepwise regression analysis was performed by taking pIC50 as dependent variable and descriptors calculated from MOE as independent variables. The statistically significant Eq. 1 ($r > 0.8$, $F >$ than reported F and $s < 0.45$) shows a positive correlation with Std_dim2 and Kier A3 and a negative correlation with SlogP_vsa1. The cross correlation between descriptors is mentioned in Table 4.

$$\mathrm{pIC50}_{\mathrm{COX\text{-}2}} = 1.281(\mathrm{Std\_dim2}) + 1.719(\mathrm{Kier\ A3}) - 0.042(\mathrm{SlogP\_vsa1}) - 0.076 \quad (1)$$

$N = 31$; $r = 0.870$; $r^2 = 0.757$; adjusted $r^2 = 0.730$; $S = 0.432$; $F_{3,27} = 28.084$; $F_{\alpha = 5\%\ 3,27} = 2.96$.

This model is capable of explaining 75.7% of the variation but the calculated activity of compound number **12** (Studentized Residual = –4.236) is showing much deviation from the observed value and hence considered as an outlier (Table 1). After excluding the compound number **12**, much more robust model with same descriptors, Eq. 2, is obtained which explains 84.9% of variance in the observed activity values. The reason for the outlier of compound number **12** is not immediately apparent. Predicted (leave-one-out), calculated and experimental activity for the training set is shown in Table 1 and graph between them is shown in Figs. 4 and 5. Leave-one-out method resulted into cross-validated q^2 of 0.80.

$$\mathrm{pIC50}_{\mathrm{COX\text{-}2}} = 0.921(\mathrm{Std\_dim2}) + 1.919(\mathrm{Kier\ A3}) - 0.037(\mathrm{SlogP\_vsa1}) - 0.238 \quad (2)$$

$N = 30$; $r = 0.922$; $r^2 = 0.849$; adjusted $r^2 = 0.832$; $S = 0.339$; $q^2 = 0.80$; $F_{3,26} = 48.807$; $F_{\alpha = 5\%\ 3,26} = 2.98$; S dep = 0.35.

Std_dim2 is three dimensional surface area, volume and shape descriptor, which depends upon structure connectivity and conformation. It is calculated as the square root of the second largest eigenvalue of the covariance matrix of the

Table 1
Structures, experimental, calculated and predicted (leave-one-activity) activity of the molecules used in training set for COX-2 inhibition

S. NO.	R1	R2	R3	IC50 $_{cox-2}$ [b,a]	pIC50$_{cox-2}$ [b]	Calculated pIC50$_{cox-2}$ [c]	Predicted pIC50$_{cox-2}$ [d]
1	CH3		OH	8.7	5.06	5.46	5.51
2	CH3	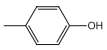	H	4.8	5.31	5.68	5.72
3	CH3	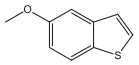	Di CH3	0.08	7.09	7.36	7.45
4	CH3	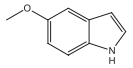	Di CH3	0.24	6.61	6.75	6.80
5	CH3	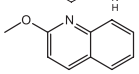	Di CH3	0.66	6.18	6.55	6.58
6	CH3	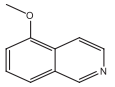	Di CH3	0.26	6.58	6.43	6.40
7	CH3	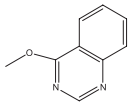	Di CH3	1.7	5.76	5.82	5.85
8	CH3		Di CH3	3.8	5.42	5.47	5.49
9	CH3	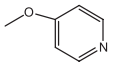	Di CH3	1	6	6.21	6.23
10	CH3	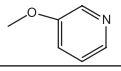	Di CH3	0.52	6.28	6.18	6.17
11	CH3	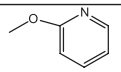	Di CH3	0.12	6.92	6.11	6.04
12	CH3	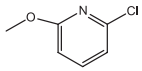	Di CH3	3.60	5.44[e]	outlier	outlier
13	CH3	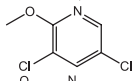	Di CH3	0.04	7.39	7.64	6.60
14	CH3	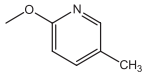	Di CH3	0.38	6.42	6.58	7.33
15	CH3	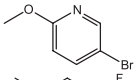	Di CH3	0.03	7.52	7.37	5.59
16	CH3	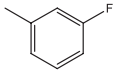	H	1.8	5.74	5.61	5.73
17	CH3	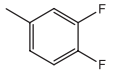	H	0.9	6.04	5.76	5.56
18	NH2	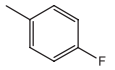	H	0.8	6.09	5.61	7.04
19	CH3	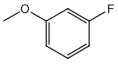	Di CH3	0.07	7.15	7.05	7.22
20	CH3	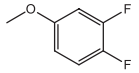	Di CH3	0.06	7.22	7.22	7.24
21	CH3	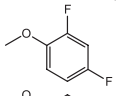	Di CH3	0.04	7.39	7.25	7.08
22	CH3	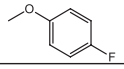	Di CH3	0.05	7.3	7.09	7.60
23	CH3	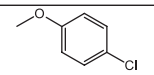	Di CH3	0.02	7.69	7.61	7.17
24	CH3	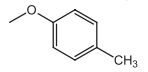	Di CH3	0.04	7.39	7.19	7.23
25	CH3	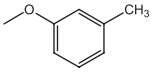	Di CH3	0.28	6.55	7.18	6.89
26	CH3	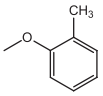	Di CH3	0.10	7	6.90	6.10
27	CH3	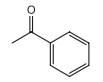	Di CH3	0.8	6.09	6.10	5.34
28	CH3	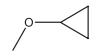	Di CH3	5.2	5.28	5.33	5.06
29	CH3	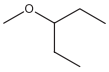	Di CH3	33	4.48	4.89	6.80
30	CH3	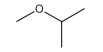	Di CH3	0.3	6.52	6.79	6.30
31	CH3	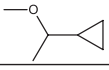	Di CH3	0.08	7.09	6.37	6.29

a-COX-2 IC50 measured as human whole blood assay, b- –Log(IC50*10^6), c-pIC50 calculated from equation 2, d-pIC50 determined by leave-one-out method, e- removed to generate equation 2.

Table 2
Structures, experimental, calculated and predicted (leave-one-out) activity of the molecules used in test set for COX-2 inhibition

S.no.	R1	R2	R3	IC50 $_{COX-2}$ [b,a]	pIC50$_{COX-2}$ [b]	Predicted pIC50$_{COX-2}$ [c]
1	CH3		H	0.53	6.27	5.15
2	CH3		Di CH3	0.86	6.06	5.51
3	CH3	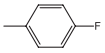	H	0.6	6.22	5.61
4	CH3	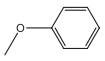	Di CH3	0.04	7.39	6.62
5	CH3		Di CH3	0.18	6.74	7.5
6	CH3		Di CH3	1.5	5.82	7.13
7	CH3		Di CH3	4.5	5.34	5.79
8	CH3	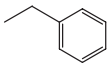	Di CH3	2.6	5.58	6.65
9	CH3	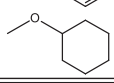	Di CH3	0.04	7.39	7.64
10	CH3		Di CH3	0.04	7.39	7.32
11	CH3		Di CH3	23	4.63	5.93
12	CH3		Di CH3	0.14	6.85	5.15

a-COX-2 IC50 measured from human whole blood, b- –Log(IC50*10^6) c-pIC50 predicted from equation 2.

atomic coordinates and is equivalent to the standard deviation along a principal component axis. The positive contribution by Std_dim2 indicates that bulky groups would be favorable for COX-2 inhibitory activity.

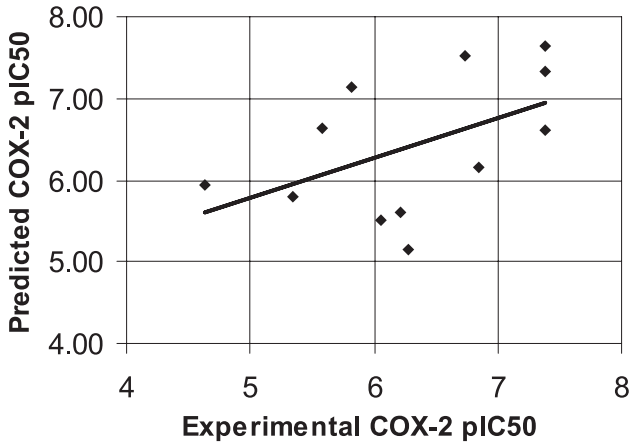

Fig. 6. Graph between experimental and predicted COX-2 inhibitory activities for test set.

Kier A3 is Kier and Hall Connectivity and Kappa Shape Index, which compares the molecular graph with minimal and maximal molecular graphs, and is intended to capture different aspects of molecular shape. Thus activities of these COX-2 inhibitors would increase with increase in Std_dim2 and Kier A3. The Eq. 2 also shows that SlogP_vsa1 is contributing negatively for biological activity. It is the subdivided surface area descriptor which is based on sum of the approximate accessible van der Waal's surface area, calculated for each atom with contribution to log of partition coefficient (octanol/water) in the range of –0.4 to –0.2 [13]. This shows that hydrophobic interaction of the inhibitors with COX-2 enzyme may influence their inhibitory activity. Equation 2 was used to predict the activity of test set (Table 2). Graph between experimental activity ($pIC50_{COX-2}$) and predicted activity for the test set is shown in Fig. 6.

The COX-2 inhibitory activity was found to show a positive correlation with lipophilicity (Eq. 3) showing 58.4% variance. MOE determines Log P as the octanol/water partition coefficient including implicit hydrogens and is calculated from a linear atom type model. COX enzyme is a membrane-based enzyme and the entry of the inhibitor in the enzyme requires that molecule should be lipophilic in nature. Thus increase in lipophilicity increases inhibitory activity.

$$pIC50_{COX-2} = 0.819(\log P) + 3.556 \quad (3)$$

$N = 30$; $r = 0.764$; $r^2 = 0.584$; adjusted $r^2 = 0.569$; $S = 0.542$; $F_{1,28} = 39.341$; $F_{\alpha = 5\%\ 1,28} = 4.20$.

To find any major differences in the properties of the molecules showing COX-2 inhibitory activity over COX-1 ($pIC50_{COX-1}$), we have derived QSAR for the available COX-1 inhibitory data (Table 3) shown in Eq. 4.

$$pIC50_{COX-1} = -0.029(Peoe\_vsa+2) - 0.013(E\_sol) + 0.044(vsa\_other) + 4.228 \quad (4)$$

$N = 18$; $r = 0.788$; $r^2 = 0.641$; adjusted $r^2 = 0.621$; $S = 0.306$; $F_{3,14} = 7.660$; $F_{\alpha = 5\%\ 3,14} = 3.34$; $q^2 = 0.401$; S dep=0.33.

Table 3
Structures, experimental, calculated and predicted (leave-one-activity) of the molecules used in training set for COX-1 inhibition

S.no.	R1	R2	R3	$IC50_{COX-1}$ [a]	$pIC50_{COX-1}$ [b]	Calculated $pIC50_{COX-1}$ [c]	Predicted $pIC50_{COX-1}$ [d]
1	CH3	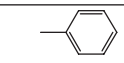	H	18.8	4.72	4.95	5.03
2	CH3	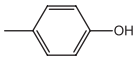	H	6.5	5.18	5.23	5.23
3	CH3	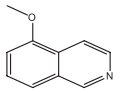	Di CH3	3	5.52	5.47	5.45
4	CH3	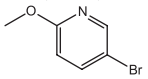	Di CH3	5.6	5.25	5.61	5.70
5	CH3	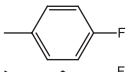	H	10	5	4.57	4.41
6	CH3	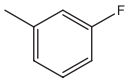	H	86	4.06	4.39	4.51
7	CH3	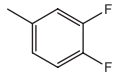	H	13	4.88	4.63	4.58
8	NH2	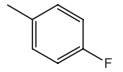	H	5.8	5.23	5.18	5.13
9	CH3	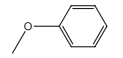	Di CH3	4.6	5.33	5.10	5.04
10	CH3	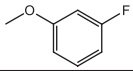	Di CH3	23.1	4.63	5.03	5.11
11	CH3	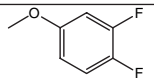	Di CH3	7.9	5.1	5.41	5.45
12	CH3	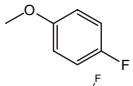	Di CH3	3.6	5.44	5.13	5.06
13	CH3		Di CH3	10.0	5	5.01	5.00
14	CH3	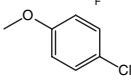	Di CH3	1.8	5.74	5.38	5.32
15	CH3	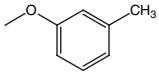	Di CH3	3.2	5.4	5.10	5.02
16	CH3	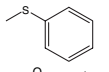	Di CH3	58	4.23	4.34	5.02
17	CH3	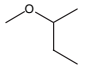	Di CH3	10	5	4.93	4.42
18	CH3	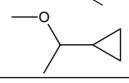	Di CH3	36	4.44	4.79	4.92

a- a-COX-1 IC50 measured from human whole blood b- –Log(IC50*10^6), c-pIC50 calculated from equation 4 d- pIC50 calculated by leave-one-out method.

The QSAR equation for COX-1 inhibitory activity shows that vsa_other, which is a pharmacophore feature descriptor and is contributing positively and E_sol the solvation energy descriptor and Peoe_vsa+2 the partial charge descriptor are contributing negatively. Vsa_other is the van der Waal's surface area of all atoms other than donor, acceptor, polar (both donor and acceptor), positive (base), negative (acid) and hydrophobic which shows that increase in van der Waal's surface area of other atoms increases inhibitory activity.

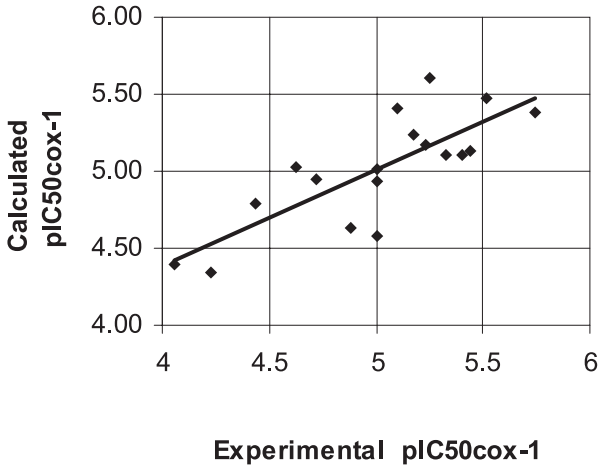

Fig. 7. Graph between experimental and calculated COX-1 inhibitory activities.

Peoe_vsa+2 is the partial charge descriptor; an electronic parameter showing that compound shows electronic interaction with COX-1 enzyme. The partial charges are calculated by Gasteiger method [14], in which charge is transferred between bonded atoms until equilibrium. Also increase in solvation energy of compound is detrimental for COX-1 activity inhibitory. Predicted (leave-one-out), calculated and experimental activity for the training set is shown in Table 3 and the graph between them is shown in Figs. 7 and 8. The cross correlation between the descriptors responsible for COX-1 inhibition is shown in Table 5.

When COX-1 inhibitory data were subjected to regression analysis with those variables which contribute to COX-2 inhibition, it was observed that they play no role in COX-1 inhibition and thus for designing selective COX-2 inhibitors (Eq. 5), contribution of Std_dim2, SlogP_vsa1, Kier A3and Log P must be taken into consideration.

$$pIC50_{COX\text{-}1} = 0.122(Std\_dim2) + 0.302(Kier\ A3) + 0.016(SlogP\_vsa1) + 2.699 \quad (5)$$

$N = 18$; $r = 0.410$; $r^2 = 0.168$; adjusted $r^2 = 0.00$; $S = 0.453$; $F_{3,14} = 0.943$; $F_{\alpha = 5\%\ 3,14} = 3.34$.

Eq. 6 shows that COX-1 inhibition does not depend on lipophilicity of the molecule.

$$pIC50_{COX\text{-}1} = 0.114(Log\ P) + 4.584 \quad (6)$$

$N = 18$; $r = 0.146$; $r^2 = 0.021$; adjusted $r^2 = 0.00$; $S = 0.463$; $F_{1,16} = 0.350$.

These initial results are promising for the development of an NSAID, which are selective COX-2 inhibitors without renal or gastric toxicity. Further research in this work could lead to the development of new selective COX-2 inhibitors.

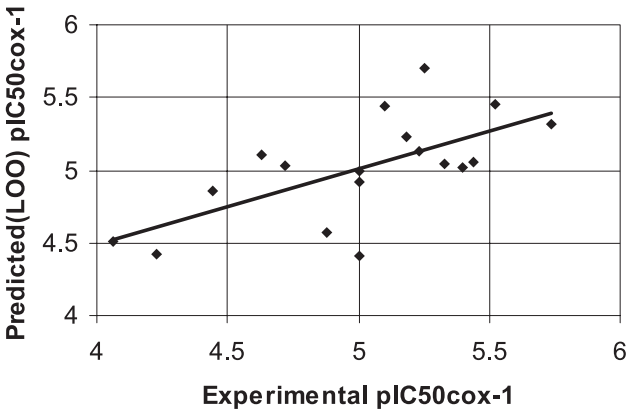

Fig. 8. Graph between experimental and predicted (leave-one-out) COX-1 inhibitory activities.

Table 5
Correlation matrix for descriptors influencing COX-1 inhibitory activity

	pIC50	Log P	Vsa_other	E_sol
pIC50	1.000			
Log P	0.146	1.000		
Vsa_other	0.627	0.573	1.000	
E_sol	–0.168	0.607	0.241	1.000
Peoe_vsa+2	–0.215	0.240	0.104	–0.147

Acknowledgements

Authors wish to thank Tata Elxsi for providing the software for the study and Head, School of Pharmacy, DAVV for providing facilities to carry out the work. S. Shahapurkar and T. Pandya wish to thank CSIR, New Delhi for providing SRF for research.

References

[1] J.R. Vane, Nature 231 (1971) 232.

[2] B. Barttisini, R. Botting, Y.S. Bakhle, Drug News Prospects 7 (1994) 501.

[3] S. Kargman, G.P. O'Neil, P.J. Vickers, J.F. Evans, J.A. Mancini, S. Jothy, Cancer Res. 55 (1995) 2356.

[4] J.J. Talley, S.R. Bertenshaw, D.L. Brown, J.S. Carter, M.J. Graneto, C.M. Koboldt, J.L. Masferrer, B.H. Norman, D.J. Rogier, B.S. Zweifel, K. Seibert, Med. Res. Rev. 3 (1999) 199.

[5] Y. Leblanc, J.Y. Gautheir, D. Ethier, J. Guay, J. Mancini, D. Riendeau, P. Tagari, P. Vickers, E. Wong, P. Prasit, Bioorg. Med. Chem. Lett. 18 (1995) 2123.

[6] T.D. Penning, J.J. Talley, S.R. Carter, P.W. Collins, S. Doctor, M.J. Graneto, L.F. Lee, J.W. Malecha, J.M. Miyashiro, R.S. Rogrs, D. Rogiers, S.S. Yu, G.D. Anderson, E.G. Burton, J.N. Cogburn, S.A. Gregory, C.M. Koboldt, W.E. Perkins, K. Seibert, A.W. Veehuizen, Y.Y. Zhang, P.C. Isakson, J. Med. Chem. 40 (1997) 1347.

[7] I.K. Khanna, H.M. Renee, W.M. Richard, X. Xu, J.F. Koszyk, J. Med. Chem. 43 (2000) 3168.

[8] W.C. Black, C. Brideau, C. Chi-Chung, S. Charleson, N. Chauret, D. Claveau, D. Ethier, R. Gordon, G. Greig, J. Guay, G. Hughes, P. Jolicoeur, Y. Leblanc, D. Nicoll-Griffith, N. Ouimt, D. Riendeau, D. Visco, Z. Wang, L. Xu, P. Prasit, J. Med. Chem. 42 (1999) 1274.

[9] (a) D.A. Nicoll-Griffith, J.A. Yergey, L.A. Trimble, J.M. Silva, N. Chauret, C. Li, J.Y. Gauthier, E. Grimm, S. Leger, P. Roy, M. Therien, Z. Wang, P. Prasit, R. Zamboni, R. Young, C. Brideau, C. Chan, J. Mancini, D. Riendeau, Bioorg. Med. Chem. Lett. 10 (2000) 2683; (b) C.K. Lau, C. Brideau, C. Chan, S. Charleson, W.A. Cromlish, D. Ethier, J.Y. Gauthier, J. Guay, S. Kargman, C. Li, P. Prasit, D. Riendeau, M. Therien, D.M. Visco, L. Xu, Bioorg. Med. Chem. Lett. 9 (1999) 3187; (c) C. Li, W.C. Black, C. Brideau, C. Chan, S. Charleson, A. Wanda, W.A. Cromlish, D. Claveau, J.Y. Gauthier, R. Gordon, G. Greig, E. Grimm, J. Guay, C.K. Lau, D. Riendeau, M. Therien, D.M. Visco, E. Wong, L. Xu, P. Prasit, Bioorg. Med. Chem. Lett. 9 (1999) 3181; (d) P. Prasit, Z. Wang, C. Brideau, C. Chan, J.Y. Gauthier, R. Gordon, S. Charleson, W.A. Cromlish, D. Ethier, J.F. Evans, A.W. Ford-Hutchinson, J. Guay, M. Gresser, S. Kargman, B. Kennedy, Y. Leblanc, J. Leger, J. Mancini, G.P. O'Neill, M. Ouellet, M.D. Percival, H. Perrier, D. Riendeau, D. Rodger, P. Tagari, P. Therien, P. Vickers, E. Wong, L. Xu, R.N. Young, R. Zamboni, Bioorg. Med. Chem. Lett. 9 (1999) 1773; (e) Y. Leblanc, P. Roy, S. Boyce, C. Brideau, C. Chan, S. Charleson, R. Gordon, E. Grimm, J. Guay, J. Leger, C. Li, D. Riendeau, D.M. Visco, J. Wang, J. Webb, J. Xu, P. Prasit, Bioorg. Med. Chem. Lett. 9 (1999) 2207.

[10] A.S. Kalgutkar, A.B. Marnett, B.C. Crews, R.P. Renmel, L.J. Marnett, J. Med. Chem. 43 (2000) 2860.

[11] A.S. Kalgutkar, S.W. Rowlinson, B.C. Crews, L.J. Marnett, Bioorg. Med. Chem. Lett. 12 (2002) 521.

[12] QSAR easy was developed in SGSITS, Indore.

[13] P. Labute, MOE LogP(Octanol/Water) Model, 1998 Unpublished, Source 3 code in $MOE/lib/svl/quasar.svl/q_logp.svl.

[14] J. Gasteiger, M. Marsili, Tetrahedron 36 (1980) 3219.